AUTHOR(S): CRAWFORD, A.R., DROUBI, M.G. and FAISAL, N.H.

TITLE: Modal acoustic emission analysis of mode-I and mode-II fracture of adhesively-bonded joints.

YEAR: 2018

Publisher citation: CRAWFORD, A.R., DROUBI, M.G. and FAISAL, N.H. 2018. Modal acoustic emission analysis of mode-I and mode-II fracture of adhesively-bonded joints. In Proceedings of the 33rd European Working Group on Acoustic Emission (EWGAE) European acoustic emission testing conference (EWGAE 2018), 12-14 September 2018, Senlis, France. Senlis: EWGAE [online], pages 218-228. Available from: http://www.ewgae2018.com/wp-content/uploads/2018/09/EWGAE-Conference-Proceedings_2018-1.pdf

OpenAIR citation: CRAWFORD, A.R., DROUBI, M.G. and FAISAL, N.H. 2018. Modal acoustic emission analysis of mode-I and mode-II fracture of adhesively-bonded joints. In Proceedings of the 33rd European Working Group on Acoustic Emission (EWGAE) on acoustic emission testing conference, 12-14 September 2018, Senlis, France. Senlis: EWGAE, pages 218-228. Held on OpenAIR [online]. Available from: https://openair.rgu.ac.uk/

EWGAE 33rd European Conference on Acoustic Emission Testing
12-14 September 2018 - Senlis - France

01 - Modal Acoustic Emission analysis of mode-I and mode-II fracture of adhesively-bonded joints

Alasdair R. Crawford, Mohamad G. Droubi, Nadimul H. Faisal

SCHOOL OF ENGINEERING, ROBERT GORDON UNIVERSITY, GARTHDEE ROAD, ABERDEEN, AB10 7GJ, UK

Abstract:

Acoustic emission (AE) testing has previously been demonstrated to be well suited to detecting failure in adhesively-bonded joints. In this work, the relationship between the fracture-mode of adhesively-bonded specimens and the acoustic wave-modes excited by their failure is investigated. AE instrumented Double-Cantilever-Beam (Mode-I fracture) and Lap-Shear (Mode-II fracture) tests are conducted on similar adhesively-bonded aluminium specimens. Linear source-location is used to identify the source-to-sensor propagation distance of each recorded hit, theoretical dispersion curves are used to identify regions of the signal corresponding to the symmetric and asymmetric wave modes, and peak wavelet-transform coefficients for the wave-modes are compared between the two fracture-modes. It is demonstrated that while both fracture-modes generate AE dominated by the asymmetric mode, the symmetric mode is generally much more significant during Mode-II fracture than Mode-I. While significant scatter and overlap in results prevents the ratio of peak-wavelet transform coefficients from being a robust single classifier for differentiation between fracture-modes in most cases, other modal analysis methods, or integration of this parameter into multi-parameter methods in future work may result in more reliable differentiation. Understanding of the wave-modes excited by the different fracture-modes also has implications for source-location, as identification of the correct modes is critical for selection of suitable wave velocities.

1. Introduction

Structural adhesive bonding is increasingly being utilized across a wide range of industries, such as the aerospace, renewable energy, marine and automotive industries. Adhesives offer a variety of advantages over more conventional mechanical fastening methods, including improved stress distribution, low weight, corrosion resistance, damping properties and the ability to join dissimilar materials and composites. They are however susceptible to defects introduced throughout manufacture and service life which can lead to catastrophic failure. These defects can include disbonds or weak “kissing” bonds, introduced by surface contamination of the adherends, voids, due to inadequate quantities of adhesive or air entrapment during lay-up, porosity, due to volatiles or entrained air, cracks, due to thermal shrinkage or applied stressed in service, and poor cure, occurring from improper mixing or inadequate thermal exposure [1].

Due to these potential defects, non-destructive testing (NDT) and condition monitoring is vital if adhesives are to be used in safety critical applications. Acoustic Emission (AE) testing has been well proven in its ability to detect adhesive failure and, particularly for large structures, the ability to provide continuous real-time monitoring over a large area is advantageous and makes AE an appealing technique to complement more conventional NDT techniques, such as ultrasound and resonant-frequency based methods.

Multiple studies of adhesively bonded joints have demonstrated the ability of AE to detect initiation and propagation of debonding and adhesive cracking through the correspondence between AE and drops in load during various fracture tests [2-5], while studies such as those by Croccolo and Cuppini [6] have demonstrated the ability to predict the final failure load of a joint, based on the acoustic emissions at lower load. Differentiation between debonding and adhesive cracking has also been achieved by Galy *et al.* [3] through clustering based on typical AE parameters, while work by Bak and Kalaichelvan [7] used peak-frequency analysis to differentiate between the failure mechanisms of adhesive failure, light fiber tear failure and fiber tear failure during lap-shear tests of composite specimens.

Dzenis and Saunders [8] successfully utilized the statistical pattern recognition software Vallen VisualClass to differentiate between Mode-I (crack opening), Mode-II (shear) and Mixed-mode fatigue failures of adhesively bonded joints. While it was demonstrated that differentiation between fracture-modes was possible, the method used, and results reported provided little insight into the fundamental differences between the recorded waveforms. The differentiation between fracture-modes is extremely valuable in the case of adhesive bonds, as there is vast disparity in the strength of bonds dependent on the loading orientation. For this reason, most adhesively bonded joints are designed to be loaded predominantly in Mode-II, and application of unexpected Mode-I loadings may therefore lead to catastrophic failure. The study will look further into the differences in AE occurring from different fracture-modes.

It has been demonstrated by Gorman [9], amongst others, that the orientation of an AE source affects the amplitudes of the wave-modes propagating from it. In-plane sources are seen to create a greater extensional/symmetric wave-mode, while out-of-plane sources are seen to create a greater flexural/asymmetric wave-mode. This finding has been previously used in modal AE analysis of composites to aid in differentiation between delamination (out-of-plane) and fiber-breakage or matrix cracking (in-plane) [10-11]. Understanding of the wave-modes generated is also crucial for accurate source location. Due to differing propagation velocities, it is critical that velocities used in calculating source-location correspond to the wave-modes for which arrival times have been detected.

The aim of this study was to investigate the wave-modes generated by Mode-I and Mode-II fracture of adhesively-bonded joints and to identify whether modal analysis has the potential to discriminate between fracture-modes in a similar manner to which it has been used to discriminate between failure mechanisms of composites. To achieve this, AE instrumented Double Cantilever Beam (DCB) (Mode-I) and Lap-Shear (LS) (Mode-II/Mixed-mode) tests have been conducted on adhesively-bonded aluminum specimens and the resulting AE analysed, using continuous wavelet-transforms and theoretical dispersion curves to identify the resulting wave-modes.

2. Experimental Setup

2.1 Specimen preparation

Both specimen types were manufactured from 3.175 mm x 50 mm HE30TF aluminium bar. Adherends were cut to 300 mm long for the DCB test, and 360 mm long for the lap shear test. Specimen widths and lengths were chosen to be as large as was practical for the available test equipment, to minimize the effects of edge-reflections in the results, and to allow significant propagation distance for the wave modes to separate through dispersion. The adhesive bonding process consisted of surface preparation, adhesive application and curing. The specimens were initially rinsed with acetone, before being abraded with P400 grade abrasive

paper, rinsed with acetone again, and then cleaned with Loctite SF 7063. Silicone grease was then carefully applied to a 60 mm long region of the DCB specimens to prevent bonding and thus create a pre-crack. Loctite EA 3430, a relatively brittle two-part epoxy adhesive, was then applied through a mixer-nozzle to the bond areas of one adherend for each of the specimens. The bond area for the DCB specimens covered the entire specimen, aside from the pre-crack, while the bond area for the shear specimens was a 50 mm x 50 mm square, located 70 mm from the ends of the adherends. Small 0.5 mm thick aluminium shims were then added into the adhesive to maintain a uniform bond thickness as the other adherends were placed on top. Once assembled, weights totaling 4 kg were added on top of each specimen and they were left to cure for a minimum of five days, at an average temperature of 19°C and humidity of about 20%.

2.2 Mechanical testing

Both types of specimen were tested using an Instron 3382 universal testing machine (UTM), controlled through BlueHill 3 software. Loading blocks were bonded to the DCB specimens to allow them to be mounted to the machine in custom made yokes. Lap shear specimens had tabs bonded to each end and were then clamped into the machine using 50 mm mechanical jaws. The loading rates used were 0.5 mm/min, based on ASTM D5528 – 01 [12], and 1.3 mm/min, based on ASTM D1002-10 [13], for the DCB and lap shear specimens respectively. DCB tests were run up to a crosshead displacement of 10 mm, while lap shear tests were run until complete failure was achieved. Each test was conducted four times to ensure repeatability.

2.3 Acoustic emission setup

Two Physical Acoustics Micro80D differential sensors were used. These were connected to a PC with a NI PCI-6115 DAQ through; Physical Acoustics 2/4/6 variable-gain pre-amplifiers (set to 60dB), an in-house built signal-conditioning unit (providing an additional 12dB gain), and a NI BNC-2120 shielded connector block. The system was operated through LabVIEW software, with the signals being recorded continuously at 2.5 MHz and saved in *.tdms format. Signal processing and analysis was conducted after testing, using MATLAB.

The sensor locations used were both on the same sides of the specimens. On the DCB specimens, as indicated in Figure 1, one sensor was located at the end of the pre-crack, and the other 10 mm from the end of the specimen. On the lap shear specimens, illustrated in Figure 2, the sensors were located either side of the bond area, at distances of 90 mm and 200 mm away from the center of the bond area. Sensors were coupled to the specimens with a layer of silicone grease and secured using aluminium adhesive tape. As well as recording AE, a video camera was used to record crack propagation for the DCB test to verify the position of the crack-front. This approach could not be used effectively for the shear specimens due to the speed of their failure.

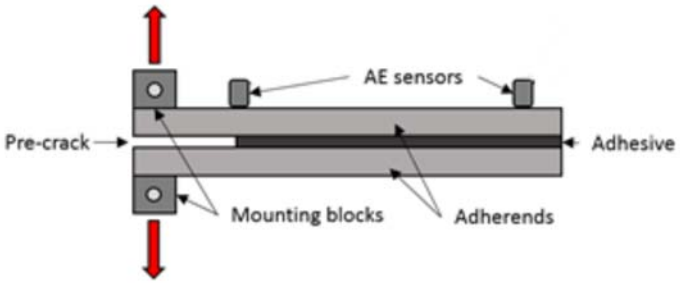

Figure 1. Double Cantilever Beam experimental schematic (not to scale)

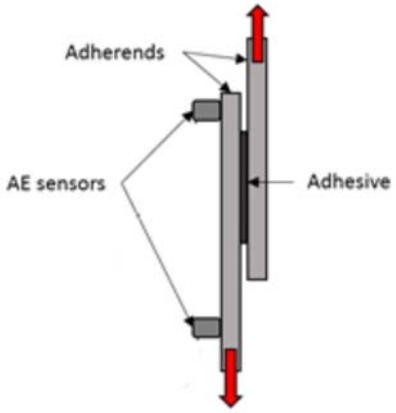

Figure 2. Lap Shear experimental schematic (not to scale)

3. Signal processing

As the system was recording continuously, the initial step was to isolate hits for further analysis and to discard the noise. This was achieved by averaging the RMS value of the signal over 200 data points, to create something similar in form to the upper wave envelope, and then applying upper and lower thresholds. Hits of significant amplitude were identified by crossings of the upper threshold. The start and end of the hit were then identified by the nearest crossings of the lower threshold before and after this point. Threshold values were set at 0.05 V and 0.15 V, chosen based on the level of noise present in the recorded signals.

The identified hits were transformed into the time-frequency domain by continuous wavelet transform. In this case the Gabor wavelet was used, as this provides the best combination of time and frequency resolution. An example of this transformation from time to time-frequency domain is illustrated in the upper panels of Figure 3. Arrival times, corresponding to the A_0 mode at 300 kHz, were determined as the first peak in the 300 kHz band of the wavelet transform to exceed 70% of the maximum WT coefficient. These arrival times, and the separation distance between the sensors, were used to estimate the linear source location of each hit, and therefore the propagation distance from the source to each of the sensors. Hits located as occurring from outwith the potential bond regions of the specimens were excluded from further analysis.

Based on the identified propagation distances, the arrival times of both the S_0 and A_0 wave-modes are calculated using the theoretical dispersion curves for the adherends (generated by Vallen Dispersion software). The central panel of Figure 3 shows these dispersion curves, modified by the propagation distance, overlaid on the wavelet transform plot of the signal. This allows certain peaks in the wavelet transform plot to be attributed to these wave-modes.

To allow quantitative analysis of the contributions of each wave-mode, the corresponding peaks within a certain frequency band were extracted. The frequency band around 300 kHz was chosen as it is close to the resonant peak of the sensor and contains significant content from both wave-modes. There is also significant enough dispersion at this frequency to differentiate between the wave-modes in the time-domain. The lower panel of Figure 3 shows

the WT coefficients in the 300 kHz band with the S_0 and A_0 peaks marked. The ratio between the amplitudes of these peaks was then used to investigate the difference between the fracture-modes. In a small number of hits the wave-modes could not be clearly identified or separated due to factors such as overlapping of hits, in such cases the hits were excluded from further analysis.

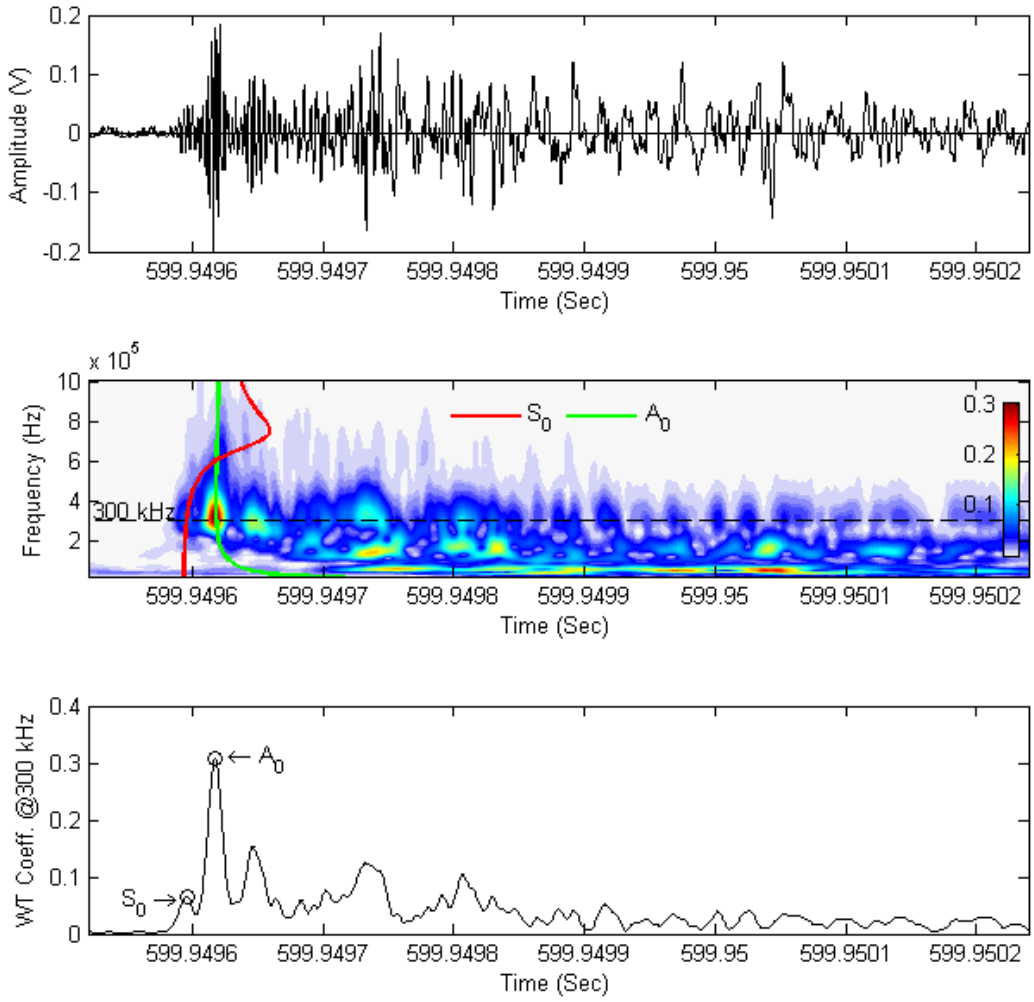

Figure 3. Example of signal-processing method. Top: Original AE signal. Middle: Wavelet Transform plot with overlaid dispersion curves indicating symmetric (S0) and asymmetric (A0) wave-modes. Bottom: Wavelet Transform coefficients for 300 kHz frequency band, with S_0 and A_0 peaks marked.

4. Results

4.1 Load results

Typical examples of the loading curves and AE source location results for the tests are shown in Figure 4. As expected, the loading characteristics of the two specimen types vary significantly. The DCB tests result in an approximately linear increase in load as the adherends deflect elastically in the pre-crack region until the maximum load is reached. This is followed by multiple small drops in load as the adhesive fails in sections, and small rises in load between these, as the adherends elastically deform again. The lap-shear tests however, exhibit an

approximately linear region of elastic deformation up to their maximum load, followed by sudden complete failure in which the adherends completely separate. The maximum loads withstood by the two specimens should be noted, as the DCB specimens withstood loads in the region of only 50 N, while maximum loads applied to the lap-shear specimens were in the region of 2000 N. This disparity highlights the potential importance of being able to discriminate between fracture-modes during condition monitoring.

4.2 Failure mechanisms

The main failure mechanism observed in all specimens was adhesive failure, with the adhesive layer separating from one adherend as the bond between adhesive layer and adherend failed, while remaining bonded to the other adherend. In the DCB specimens, and to a lesser extent in two of the lap-shear specimens, some adhesive cracking was also found. In some regions the adhesive failure would occur at the interface with the upper adherend, and in other regions it would occur at the lower adherend. The result being that the adhesive layer cracked between these regions, allowing sections of the adhesive to remain attached to either adherend. Figure 5 shows annotated examples of the failure mechanisms present in both types of specimen.

4.3 Acoustic emission source locations

In both specimen types, a small number of hits were recorded during the initial linear portion of the loading. Most hits however, correspond to significant drops in load as the adhesive fails. In the DCB specimen hits are spread throughout the test as crack slowly propagates through the specimen, whereas in the lap-shear test, AE activity is concentrated around the moment of final failure. The AE source locations identified in the DCB tests generally correspond well with the visually observed crack-front recorded with the video-camera, with the hits initially being centered around the tip of the 60 mm pre-crack and then progressing further along the specimens as the crack opens. While the AE source location results generally correspond well, there is some variation and scatter which is believed to be due to a combination of the following factors; the crack-front will not be uniform due to the inhomogeneous bond quality, so the location of the crack-front recorded at one side will not necessarily be accurate through the entire specimen width. The use of a linear source-location method, as opposed to 2D or 3D, will also generally result in a small level of error as not all hits will occur directly between the sensors. In the lap-shear specimens hits are concentrated within the bond area, as would be expected, although some hits are identified as occurring out with the bond area. This may again be due to the limitations of linear source-location but may also be due in some cases to the incorrect identification of arrival times due to interference between overlapping hits, a problem which can also occur in the DCB specimens but is much more prominent in the lap-shear tests due to the limited time in which the hits all occur.

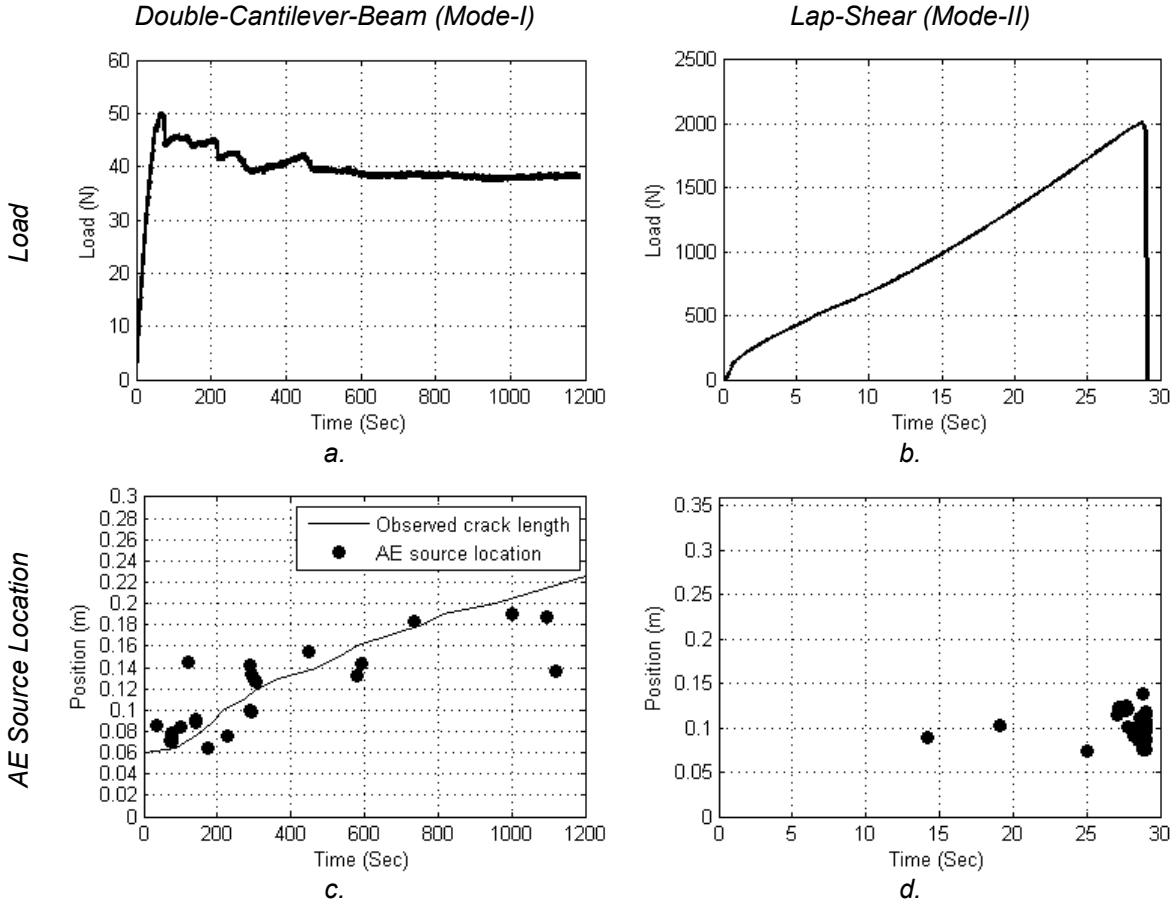

Figure 4. Examples of loading curves and source locations. (a) Loading of DCB test. (b) Loading of lap-shear test. (c) AE source location and visually observed crack length for DCB test. (d) AE source location for lap-shear test.

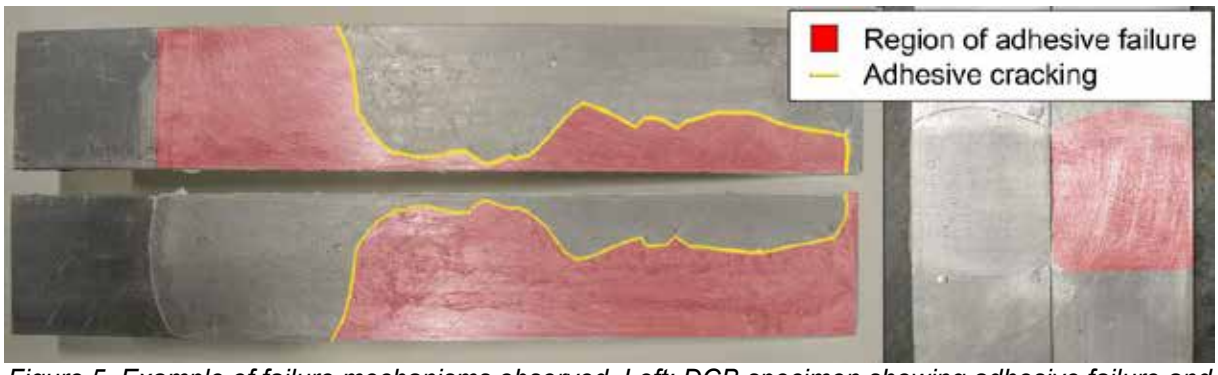

Figure 5. Example of failure mechanisms observed. Left: DCB specimen showing adhesive failure and cracking of the adhesive layer. Right: Lap-shear specimen showing only adhesive failure.

4.4 Modal acoustic emission analysis

The resulting ratios of the peak wavelet-transform coefficients corresponding to the S_0 and A_0 wave-modes are presented in Figure 6. Both fracture-modes can result in a wide range of S_0/A_0 ratios being generated. For the DCB tests, values range from 0.0169 to 0.4178 with an overall

mean and standard deviation of 0.085 and 0.0848 respectively. Lap-shear tests produced values ranging from 0.0616 to 0.7197 and with an overall mean and standard deviation of 0.1902 and 0.1425.

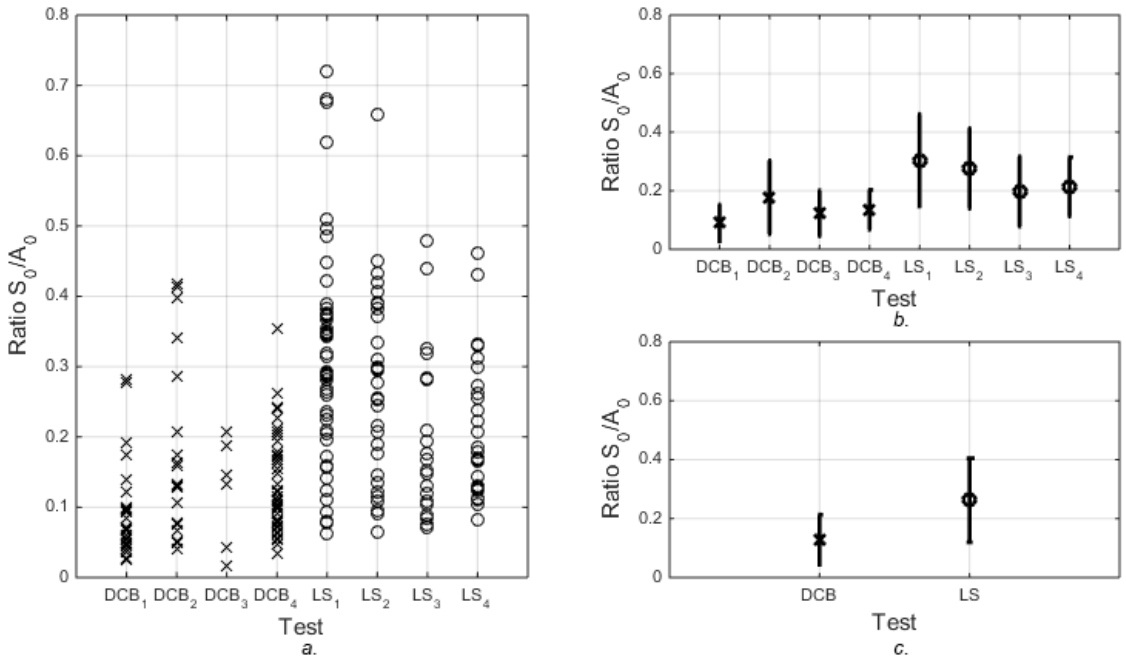

Figure 6. Ratios of peak wavelet-transform coefficients at 300 kHz corresponding to S_0 and A_0 wave-modes. (a) All hits analysed. (b) Mean and std. deviation for each test. (c) Overall mean and std. deviation for the two test types.

5. Discussion

The WT coefficient peak ratios show that in both tests the A_0 mode is dominant and that there is significant overlap between the sets of results. There is however a clear trend indicating that the S_0 mode is generally greater in the Mode-II lap-shear tests than in the Mode-I DCB tests. This result appears to be in line with previous work, as Mode-I failure creates a clear out-of-plane source, very similar to the delamination of composites, which has previously been shown to create a dominant A_0 component.

While the loading in the Mode-II test is applied in-plane with respect to the adherends, any failure occurring at the interface with the adhesive is occurring at the surface of the adherend rather than near the mid-plane, as can be the case for other in-plane sources previously investigated, such as fiber-failure or matrix cracking in composites. It has been previously demonstrated by Hamstad *et al.* [14] that while a signal generated by an in-plane source located on the mid-plane will be dominated by the symmetric mode, the same source, applied away from the mid-plane, can create a signal dominated by the asymmetric mode. This provides some explanation as to why both fracture-modes result in signals dominated by the asymmetric mode, despite the loading orientation. Additionally, a lap-shear test is technically not a pure Mode-II test, while the loading is predominantly in shear, bending of the adherends can result in a small Mode-I crack-opening component, making it Mixed-mode and potentially contributing further to the generation of the A_0 mode.

As both fracture-modes have a significantly higher amplitude A_0 than S_0 mode, a suitably chosen threshold can be used to consistently select the arrival time of the A_0 mode, without risk of accidental selection of the S_0 arrival time. If the Mode-II tests had resulted in a greater S_0 component, then a more sophisticated method would be necessary to select arrival times and calculate source locations.

The results presented by Dzenis and Saunders [8], analysed using Vallen VisualClass, clearly demonstrated the possibility to differentiate between fracture-modes using AE, they did not however provide much insight into the fundamental differences in the signals which allowed this differentiation. The results presented in this work indicate that it is likely that the difference in wave-modes excited during their tests will have been one of the significant factors contributing to the differentiation which was achieved, while other differences may have also occurred from features such as the specimen geometries causing variation in attenuation and reflections. An increased understanding of these factors allowing differentiation will be beneficial if attempts are made to utilize these techniques on full scale structures, rather than small laboratory specimens, as any method used will need to suitably account for the dispersion, attenuation and reflection which will be present in larger structures with potentially irregular geometries.

The use of the WT peak ratio as a classifier to differentiate between fracture-modes may be feasible when considering multiple hits, i.e. an entire test, however due to significant variation between hits, and the overlap between tests, it would not be possible in most cases to identify fracture-mode based on a single hit. Future work should therefore consider either; other methods to assess the modal content of the signals which may yield clearer discrimination, or, combining this parameter with others to form a more robust method of discrimination.

Differentiation between hits occurring from the adhesive failure and cracking of the adhesive layer has not yet been attempted within this study, and it is recognized that results for each test may include hits from both failure mechanisms which may exhibit different characteristics. Future work should address this issue by conducting tests capable of isolating each of these failure mechanisms to identify the defining characteristics of AE occurring

6. Conclusion

The aim of this study was to investigate, for the first time, the AE wave-modes generated by Mode-I and Mode-II fracture of adhesively-bonded joints (aluminium metal-to-metal) and to identify whether modal analysis has the potential to discriminate between fracture-modes in a similar manner to which it has been used to discriminate between failure mechanisms of composites. Differentiation between fracture-modes is particularly important in adhesive joints due to the vast disparity in strength between joints in Mode-I and Mode-II loading, assessment of loading conditions through AE could therefore provide a very useful tool for structural health monitoring. Understanding of the wave-modes generated by different fracture-modes is also important for accurate source location. Due to the differing propagation velocities of the modes, it is critical that the velocity used in source location calculations corresponds to the wave-mode for which arrival times have been detected. From the work conducted, the following has been concluded:

- Use of linear source location to identify propagation distances and theoretical dispersion curves to identify arrival times, has successfully identified regions of the time-frequency domain corresponding to the fundamental S_0 and A_0 modes.

- Modal analysis, based on investigation of the amplitude-ratio of peaks in the continuous wavelet-transform corresponding to the S_0 and A_0 modes, has revealed clear differences between Mode-I and Mode-II/Mixed-mode fracture. While signals from both fracture-modes are dominated by the A_0 mode, the S_0 mode is generally greater in the Mode-II tests than in the Mode-I.

- As the amplitude of the A_0 mode is consistently higher than that of the S_0 mode, a suitably chosen threshold can be used as a reliable method to select the arrival time of the A_0 mode for the purposes of source location.

- Analysis of the amplitude-ratio of wavelet-transform peaks corresponding to the wave-modes has been demonstrated to reveal differences between the fracture-modes when considering each test. However, due to the variation between hits within each test, and the overlap between results from the two test types, it is generally not possible to distinguish between fracture-modes based on a single hit. Future work should therefore focus on investigation of other methods to assess modal content of the signals or on utilizing the wavelet peak ratio in combination with other parameters to provide a more robust classifier.

References:

[1] R. D. Adams, "Nondestructive Testing," in *Handbook of Adhesion Technology*, Oxford, Springer, 2011, pp. 1050-1067.

[2] M. G. Droubi, A. Stuart, J. Mowat, C. Noble, A. K. Prathuru and N. H. Faisal, "Acoustic emission method to study fracture (Mode-I, II) and residual strength characteristics in composite-to-metal and metal-to-metal adhesively bonded joints," *The Journal of Adhesion,* 2017.

[3] J. Galy, J. Moysan and A. Y. N. M. N. El Mahi, "Controlled reduced-strength epoxy-aluminium joints validated by ultrasonic and mechanical measurements," *International Journal of Adhesion and Adhesives,* vol. 72, pp. 139-146, 2017.

[4] M. G. Droubi, J. Mcafee, H. R. C, S. Walker, C. Klaassen, A. Crawford, A. K. Prathuru and N. H. Faisal, "Mixed-mode fracture characteristics of metal-to-metal adhesively bonded joints: experimental and simulation methods," in *Structural Integrity Procedia*, Funchal, 2017.

[5] K. Senthil, A. Arockiarajan and R. Palaninathan, "Experimental determination of fracture toughness for adhesively bonded composite joints," *Engineering Fracture Mechanics,* no. 154, pp. 24-42, 2016.

[6] D. Croccolo and R. Cuppini, "A methodology to estimate the adhesive bonding defects and the final releasing moments in conical joints based on the acoustic emissions technique," *International Journal of Adhesion & Adhesives,* no. 26, pp. 490-497, 2006.

[7] M. K. Bak and K. Kalaichelvan, "Evaluation of Failure Modes of Pure Resin and Single Layer of Adhesively Bonded Lap Joints Using Acoustic Emission Data," *Transactions of the Indian Institute of Metals,* no. 68, pp. 73-82, 2015.

[8] A. Dzenis and I. Saunders, "On the possibility of discrimination of mixed mode fatigue fracture mechanisms in adhesive composite joints by advanced acoustic emission analysis," *International Journal of Fracture,* no. 117, pp. 23-28, 2002.

[9] M. R. Gorman, "AE Source Orientation by Plate Wave Analysis," *Journal of Acoustic Emission,* vol. 9, no. 4, pp. 283-288, 1991.

[10] J. Martínez-Jequier, A. Gallego, E. Suárez, F. J. Juanes and Á. Valea, "Real-time damage mechanisms assessment in CFRP samples via acoustic emission Lamb wave modal analysis," *Composites Part B: Engineering,* vol. 68, pp. 317-326, 2015.

[11] M. Surgeon and M. Wevers, "Modal analysis of acoustic emission signals from CFRP laminates," *NDT & E International,* no. 32, pp. 311-322, 1999.

[12] ASTM International, "D5528-01 Standard Test Method for Mode I Interlaminar Fracture Toughness of Unidirectional Fiber-Reinforced Polymer Matrix Composites," ASTM International, West Conshohocken, 2007.

[13] ASTM International, "D1002-10 Standard Test Method for Apparent Shear Strength of Single-Lap-Joint Adhesively Bonded Metal Specimens by Tension Loading (Metal-to-Metal)," ASTM International, West Conshohocken, 2010.

[14] M. A. Hamstad, A. O'Gallagher and J. Gary, "A wavelet transform applied to acoustic emission signals: Part 1: Source Identification," *Journal of Acoustic Emission,* no. 20, pp. 39-61, 2002.